Broken Symmetry and the Formation of Hot-Electron Domains in Real-Space-Transfer Transistors

Serge Luryi and Mark R. Pinto
AT&T Bell Laboratories, Murray Hill, New Jersey 07974
(Received 20 May 1991)

Real-space-transfer (RST) transistors are studied theoretically. In a symmetric configuration, with no voltage applied between the channel electrodes, we find anomalous steady states in which the RST is driven by the fringing field from the collector electrode. Some of these states are unconditionally stable and hence accessible experimentally. Our study elucidates the formation of hot-electron domains, which is shown to be a discontinuous process that passes the control of electron heating from the drain to the collector. Multiply connected current-voltage characteristics are predicted.

PACS numbers: 73.50.Fq, 73.40.Kp, 73.50.Lw

The concept of real-space transfer (RST) refers to a process in which electrons in a narrow semiconductor layer are heated by a parallel field and spill over an energy barrier into adjacent layers [1,2]. A number of high-speed electronic and optoelectronic devices have been proposed based on this principle [3–7]. The generic RST transistor [8] is a three-terminal device (see the inset to Fig. 1) consisting of a channel with two contacts, S and D, and an individually contacted collector C, separated from the channel by a heterojunction barrier. In the normal operation, the channel electrons are heated by the lateral field due to a voltage V_D applied between S and D. The resultant RST leads to highly nonlinear effects, including a strong negative differential resistance (NDR) with sharp steps, indicative of an internal switching and the formation of high-field domains [4,9,10]. These processes are not well understood, even though RST transistors have been extensively studied, both experimentally and theoretically [11].

The RST transistor is symmetric with respect to reflections in the midplane normal to channel. Hence states of the device at an external bias $[V_D, V_C]$ are related to those at $[-V_D, (V_C - V_D)]$. In particular, states at $V_D = 0$ must either be symmetric or possess broken-symmetry partners. An important discovery of the present work is the existence of a number of such states, some of which are not only stationary but also *stable* with respect to small perturbations. In these "anomalous" states [12], the electron heating is due to the fringing field from the collector electrode. Our study shows that the formation of hot-electron domains at $V_D > 0$ represents a transition to a collector-controlled state that is continuously related to one of the anomalous states at $V_D = 0$.

The tool of our study is a numerical simulation of the hot-electron transport in a three-terminal RST structure. Details of the program and computational methods are described elsewhere [13,14]. The analysis is based on the solution of a set of coupled partial differential equations, including Poisson's equation and expressions [15] for current continuity and energy balance, in a two-dimensional sample, subject to boundary conditions at the three electrodes. Models for the local hot-electron mobility $\mu(T_e)$ and the energy relaxation time $\tau_E(T_e)$ are chosen so that in a uniform electric field F, one obtains given velocity-field $v(F)$ and temperature-field $T_e(F)$ characteristics. The current density is assumed to consist of drift ($en\mu\nabla V$) and thermodiffusion ($\mu\nabla[nkT_e]$) components, where n is the electron concentration and V the electrostatic potential. The quasi-Fermi level and T_e are assumed continuous at all heterostructure interfaces; this implies that the RST current density is thermionic and included self-consistently in the continuity equations.

The results presented correspond to a specific choice of an InGaAs/InAlAs heterostructure, lattice-matched to InP. In particular, the height of the $In_{0.52}Al_{0.48}As$ barrier, separating the $In_{0.53}Ga_{0.47}As$ channel and collector layers, is taken equal 0.5 eV. In order to disentangle our results from NDR effects arising from the momentum-space transfer, we have chosen the $v(F)$ dependence in a simple form [16], $v = \mu_0 F[1 + (\mu_0 F/v_{sat})^2]^{-1/2}$, parametrized by the low-field mobility μ_0 and the saturation velocity v_{sat}. Our results remain qualitatively similar for a more realistic $v(F)$ model, appropriate for InGaAs. To further simplify the discussion, we have excluded the phenomena of impact ionization and tunneling. In the examples below, we assumed the lattice temperature $T = 300$ K, a constant (T_e independent) diffusivity [17] $D = \mu_0 kT/e$, and a $\mu_0(N_D)$ that is a function of the local ionized impurity concentration [in the low-doped ($N_D = 10^{16}$ cm^{-3}) channel and undoped barrier regions $\mu_0 \approx 10^4$ cm^2/V s]. We have performed a number of simulations, varying the geometry (channel length L_{ch} and barrier thickness d_B), the transport parameter v_{sat}, and the external bias conditions.

Figure 1 illustrates a time-dependent simulation, in which both the S and D electrodes are kept grounded, while V_C is linearly ramped from 0 to $V_C = 2$ V. Depending on the ramping time τ the device settles in one of two states: for $\tau > \tau_{cr}$ it is the normal [12] state, whereas for $\tau < \tau_{cr}$ the steady state carries a large RST current [Fig. 1(a)]. The critical ramping speed is determined by the rate at which the increasing fringing field [Fig. 1(b)] is screened by channel electrons. The relevant parameter is

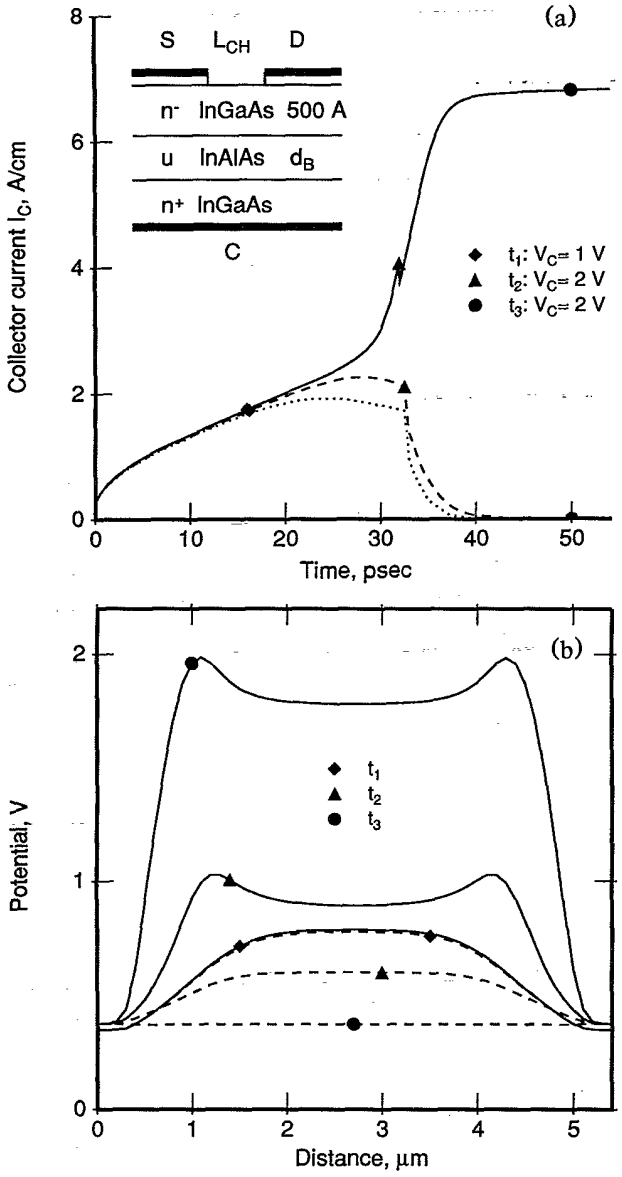

FIG. 1. Time-dependent simulation of a real-space-transfer transistor with $L_{ch}=5$ μm, $d_B=0.2$ μm, and $v_{sat}=10^7$ cm/s. The collector voltage is ramped linearly from $V_C=0$ at $t=0$ to $V=2$ V at $t=\tau$. The results are plotted for two situations: $\tau=32.0$ ps $<\tau_{cr}$ (solid lines) and $\tau=32.5$ ps $>\tau_{cr}$ (dashed lines). (a) Collector current $I_C(t)$. Inset: Cross section of the device structure. Dotted curve corresponds to the absence of a RST (pure displacement current); it is obtained by artificially increasing the barrier height. (b) Potential distribution $V(x)$ along the channel at selected times.

the displacement current ($\propto dV/dt$) compared to a transient current ($\propto v_{sat}$) in the channel [18]. The value of $\tau_{cr}\approx 32.3$ ps roughly corresponds to the time of electron travel from S and D contacts to the middle of the channel.

Starting from the two stationary states at $V_D=0$, we were able to determine the characteristics $I_D(V_D)$ and

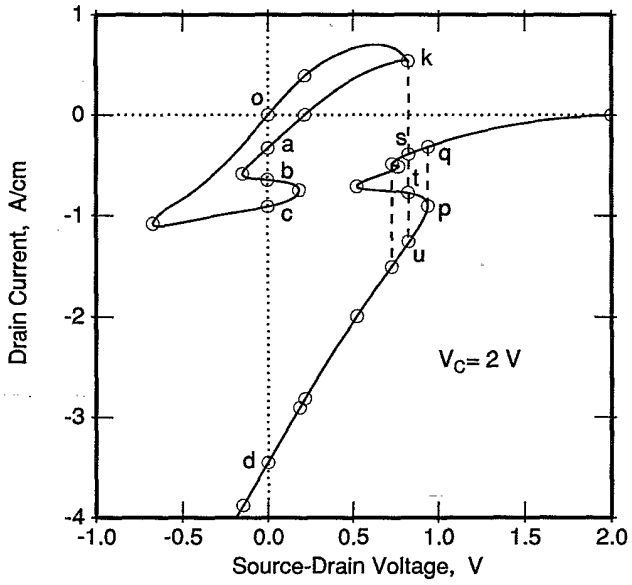

FIG. 2. Current-voltage characteristics obtained by the continuation method. Circles mark the states where the distribution of internal fields has been closely examined; states discussed in this Letter are labeled. Dashed lines indicate the transitions studied by transient simulations.

$I_C(V_D)$ at a fixed collector voltage $V_C=2$ V relative to the S electrode. Using a predictor-corrector continuation method [13], we are able to trace arbitrarily shaped, connected components of the characteristic, starting from any established state within each component. The curves in Fig. 2 correspond to the locus of points in the (V_D,I_D) plane for which the device has a steady state at a given V_C. To our knowledge, the displayed $I_D(V_D)$ dependence represents the first example of a multiply connected current-voltage characteristic. The known NDR devices may exhibit multivalued functions in the $I(V)$ dependence (e.g., the *pnpn* diode), in the $V(I)$ dependence (the Esaki tunnel diode, the Gunn diode), or even in both (the thyristor [13], the resonant tunnel diode in the intrinsic-bistability range [19])—but these can always be traced as a continuous curve in the (V,I) plane.

Points, separated by a finite distance on a (V,I) plane, correspond to macroscopically distinct states of the device. Any transition between disconnected components of the graph requires a global redistribution of the state fields [i.e., all the fields $n(\mathbf{r})$, $T_e(\mathbf{r})$, $V(\mathbf{r})$, etc.] corresponding to the formation or repositioning of high-field, high-temperature domains in the structure. Such a redistribution, reminiscent of a phase transition, is forced as V_D increases beyond the rightmost point (k) of the bounded graph component. The potential profiles $V(x)$ along the channel—before and after the transition—are shown in Fig. 3. Of the three collector-controlled states, s, t, and u, corresponding to the same ($V_D\approx 0.82$ V) external bias as the state k, two (s and u) are stable. The actual transition occurs into the state u which has

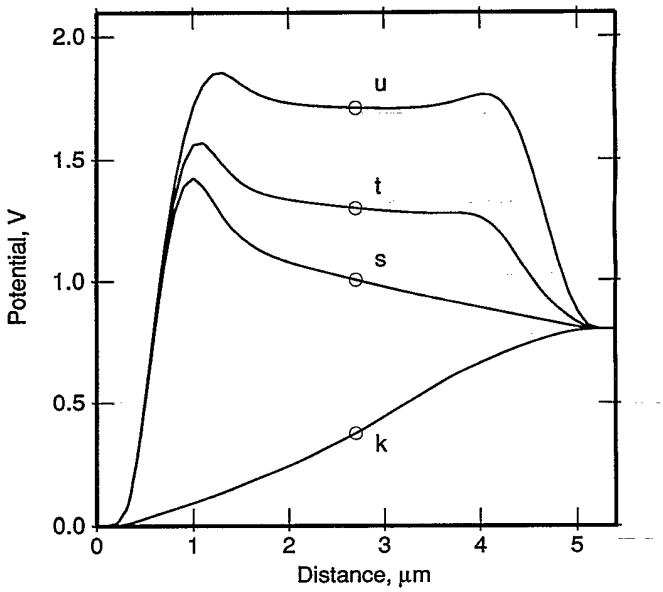

FIG. 3. The channel potential profile $V(x)$ in states k, s, t, and u, corresponding to the same external bias ($V_C=2$ V, $V_D=0.8246$ V).

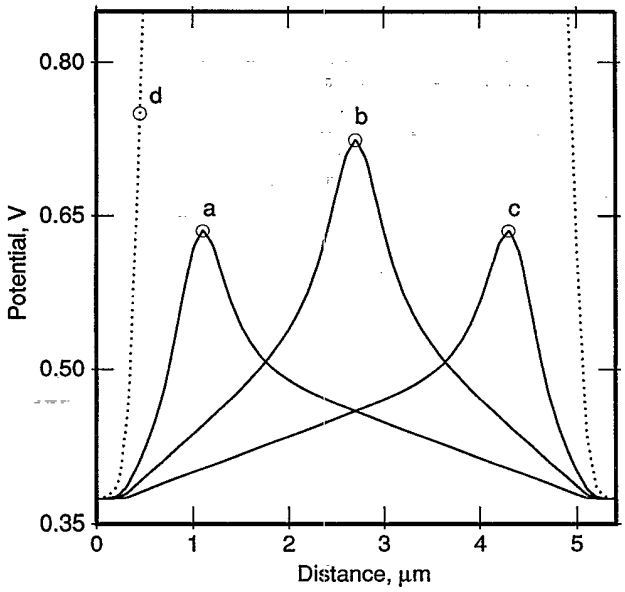

FIG. 4. The channel potential in the four anomalous states at $V_D=0$. Solid lines correspond to states on the bounded component of the graph in Fig. 2, and dotted lines to the unbounded component.

the highest value of the collector current. This has been ascertained by a time-dependent simulation in which the initial state k was perturbed by a small step $V_D(k) \rightarrow V_D(k)+\delta V_D$. The hot-electron domains in the state u are characterized by a strong field concentration, accompanied by a dramatic rise in T_e. The electron concentration in the domain is depleted so that the collector field remains unscreened and the local potential goes below that of the drain [20], resulting in a negative I_D.

Increasing V_D beyond $V_D(u)$ results in a smooth evolution of the field distribution inside the device—until another instability is encountered at $V_D \approx 0.94$ V and the device switches between states p and q. On the way back (decreasing V_D), the device remains stable at s, but at $V_D \approx 0.73$ V (the small knee in Fig. 2) it suffers another instability and goes over into a high-current state similar to u. The large knee at $V_D \approx 0.52$ V is in an unstable region and cannot be reached. On the other hand, all states on the high-current branch p-u-d of the collector-controlled component are perfectly stable. Of particular interest is the state d that we had arrived at (Fig. 1) in rapid ramping of V_C at $V_D=0$. Stability of the p-u-d branch suggests that d is experimentally accessible by a quasistatic variation of V_D at fixed V_C.

In addition to the normal state o and the anomalous state d, Fig. 2 reveals three other anomalous states (a, b, and c) at $V_D=0$. The profiles $V(x)$ along the channel in these states are shown in Fig. 4. It is clear that because of the nonlinear nature of the problem, the actual stationary states may not transform according to irreducible representations of the symmetry group of the equations governing the device behavior at $V_D=0$. Thus, states a and c under reflection transform into each other, even though the group has only one-dimensional linear representations. On the other hand, states o, b, and d are symmetric. Biasing the D electrode with respect to S breaks the reflection symmetry and allows a continuous transformation between states of different symmetry on the loop.

Of the fives states at $V_D=0$ only two (o and d) are stable with respect to small perturbations. This has been ascertained by following the evolution of states in the vicinity of the steady states at $V_D=0$. In these simulations, the initial states $a\pm$, $b\pm$, and $c\pm$ have been assumed to coincide with a state on the loop displaced from a, b, and c, respectively, by an infinitesimal voltage $\delta V_D=\pm 10$ meV. Even though these states are virtually indistinguishable from the corresponding stationary ones, we found that $a+$, $b-$, and $c-$ evolved into o, while $a-$, $b+$, and $c+$ into d. The instability of states a and c is associated with a NDR in the $I_C(V_C)$ dependence, $(\partial I_C/\partial V_C)_{a,c}<0$, and that of b with both $(\partial I_C/\partial V_C)_b<0$ and $(\partial I_D/\partial V_D)_b<0$. The instabilities develop rapidly [18] and result in either the formation of a stable hot-electron domain or its complete quench due to the screening by channel electrons.

We believe the phenomena that occur at $V_D=0$ capture the essential physics associated with the RST domains in general. Hot-electron domains are formed when the finite supply rate of electrons to a "hot spot" is exceeded by the RST flux from that spot. The supply is limited by the electronic transport along the channel. Besides the geometry and the barrier height, v_{sat} is the most relevant parameter for the domain formation. The depleted domains unscreen the fringing field ("normally"

[12] screened by channel electrons) and the RST becomes collector controlled. States of a multiterminal RST device under general bias are "adiabatically" connected to the anomalous states of the symmetric configuration at $V_D=0$. Either the distribution of internal fields in the anomalous states is fully symmetric or these states form a set of partners and transform into one another under the symmetry operations [21].

All steady-state results reported in this Letter correspond to a fixed bias $V_C=2$ V. We have also performed an extensive mapping of the device $I_{D,C}(V_D,V_C)$ phase space, varying the geometry and assumed transport parameters. Slicing the $I_D(V_D,V_C)$ surface at different V_C, we find $I_D(V_D)$ curves of different topologies, with disconnected loops and possible self-intersections [22]. We believe the loops and folds are responsible for the steps observed [10] in the characteristics of RST transistors. The internal fields $n(\mathbf{r})$, $T_e(\mathbf{r})$, $V(\mathbf{r})$, etc., evolve smoothly along a connected $I_D(V_D)$ trajectory and do not signal the approach of a switching transition. Phase-space mappings successfully give the global type of information. Moreover, they give an unerring guess as to the *stability* of a given state, subsequently supported by costlier transient simulations.

The existence of a stable anomalous state d is obviously a necessary (though insufficient) condition for the multiply connected topology of the $I_D(V_D)$ characteristic. As discussed above, it results when the competition between RST and screening of the fringing collector field is resolved in favor of RST. Precisely when this happens depends on the transport parameters assumed and the structure geometry. We stress, however, that *qualitatively* the occurrence of these novel anomalies is a consequence of the hot-electron injection only and can be reproduced in *any* transport model that allows channel electrons to be heated and self-consistently includes the RST flux.

[1] Z. S. Gribnikov, Fiz. Tekh. Poluprovodn. **6**, 1380 (1972) [Sov. Phys. Semicond. **6**, 1204 (1973)].

[2] K. Hess, H. Morkoç, H. Shichijo, and B. G. Streetman, Appl. Phys. Lett. **35**, 469 (1979).

[3] A. Kastalsky and S. Luryi, IEEE Electron Dev. Lett. **4**, 334 (1983).

[4] S. Luryi and A. Kastalsky, Superlattices Microstr. **1**, 389 (1985).

[5] K. Hess, Festkörperprobleme **25**, 321 (1985).

[6] S. Luryi, P. Mensz, M. Pinto, P. A. Garbinski, A. Y. Cho, and D. L. Sivco, Appl. Phys. Lett. **57**, 1787 (1990).

[7] S. Luryi, Appl. Phys. Lett. **58**, 1727 (1991).

[8] S. Luryi, A. Kastalsky, A. C. Gossard, and R. H. Hendel, IEEE Trans. Electron Dev. **31**, 832 (1984).

[9] I. C. Kizillyalli and K. Hess, J. Appl. Phys. **65**, 2005 (1989).

[10] P. M. Mensz, S. Luryi, A. Y. Cho, D. L. Sivco, and F. Ren, Appl. Phys. Lett. **56**, 2563 (1990); **57**, 2558 (1990).

[11] Review of the recent work and general references on real-space-transfer devices can be found in S. Luryi, Superlattices Microstr. **8**, 395 (1990).

[12] In the "normal" state of the device, for $V_D=0$, the collector draws only a minimal current, determined by the height of the barrier and the temperature. In this state a variation of V_C has the sole effect of changing capacitively, as in a field-effect transistor, the electron concentration in the channel.

[13] W. M. Coughran, Jr., M. R. Pinto, and R. K. Smith, J. Comput. Appl. Math. **26**, 47 (1989).

[14] M. R. Pinto, W. M. Coughran, Jr., C. S. Rafferty, R. K. Smith, and E. Sangiorgi, in *Computational Electronics,* edited by K. Hess *et al.* (Kluwer, Boston, 1990), p. 3.

[15] These expressions are similar to those proposed by R. Stratton, Phys. Rev. **126**, 2002 (1962). The precise equations used have been listed by M. R. Pinto, in "ULSI Science and Technology", edited by J. Andrews and G. K. Celler [Electrochem. Soc. Proc. (to be published)].

[16] D. M. Caughey and R. E. Thomas, Proc. IEEE **55**, 2192 (1967).

[17] K. Hess and C.-T. Sah, IEEE Trans. Electron Dev. **25**, 1399 (1978); G. Baccarani and M. R. Wordeman, Solid State Electron. **28**, 407 (1985). The constant-diffusivity assumption together with the $v(F)$ curve uniquely determine $\tau_E(T_e)$, $\mu(T_e)$, and the dimensionless coefficient in the Wiedemann-Franz heat-conduction term [15].

[18] Transient simulations are discussed in greater detail in a separate publication [S. Luryi and M. R. Pinto, Semicond. Sci. Technol. (to be published)].

[19] V. J. Goldman, D. C. Tsui, and J. E. Cunningham, Phys. Rev. Lett. **58**, 1256 (1987).

[20] This effect ($I_D<0$ for $V_D>0$) had been seen experimentally in RST transistors. However, it was usually attributed to spurious effects and never reported. Qualitatively, the behavior of I_D with increasing V_D is in agreement with experiment.

[21] This type of analysis is likely to prove very potent with devices of more complicated symmetry, e.g., the RST logic elements [6,7] that have three top electrodes arranged with the symmetry of C_{3v}.

[22] Of course, all this structure goes away if we suppress the RST by increasing the barrier height [cf. Fig. 1(a)] or shortening the energy relaxation time in the transport equations. The complete phase-space mappings will be reported at the 1991 International Electron Device Meeting, Washington, DC [M. R. Pinto and S. Luryi, in 1991 IEDM Technical Digest (to be published)].